US Army Corps
of Engineers®
Engineer Research and
Development Center

Sound Propagation Through a Forest:

A predictive model

Michael White and Michelle Swearingen   November 2004

20050118 005

BEST AVAILABLE COPY

ERDC/CERL MP-04-3
November 2004

Sound Propagation Through a Forest: A predictive model

Michael White and Michelle Swearingen

Construction Engineering Research Laboratory
PO Box 9005
Champaign, IL 61826-9005

Final Report

Approved for public release; distribution is unlimited.

Prepared for   U.S. Army Corps of Engineers
                 Washington, DC 20314-1000

Under   Work Unit # CNN-T114

ABSTRACT: Previous attempts at modeling sound propagation through a forest have largely neglected the effects of a sound speed profile. This paper presents a PE-based sound propagation model that includes forest effects. In addition to a simplified but realistic sound speed profile, the model includes ground impedance effects, bulk attenuation due to multiple scattering by tree trunks and canopy, and the usual spherical spreading and atmospheric absorption.

Contents

Preface

Sound propagation through a forest: a predictive model

Michelle E. Swearingen and Michael J. White
US Army Engineer Research and Development Center
Construction Engineering Research Laboratory
2902 Farber Drive
Champaign, IL 61822 USA
phone: (217)352-6511
email: michelle.e.swearingen@erdc.usace.army.mil
michael.j.white@erdc.usace.army.mil

Abstract

Previous attempts at modeling sound propagation through a forest have largely neglected the effects of a sound speed profile. This paper presents a PE-based sound propagation model that includes forest effects. In addition to a simplified, but realistic, sound speed profile, the model includes ground impedance effects, bulk attenuation due to mulitple scattering by the tree trunks and canopy, and the usual spherical spreading and atmospheric absorption. The model is compared to acoustic measurements taken in July 2002 at Lone Star Army Ammunition Plant in Texarkana, TX. In the measurement, Composition C-4 explosions were used as the acoustic source. Acoustic measurements were make at 174 m and 1400 m from the source in the forest, and 174 m from the source in an open field. Measured tree trunk diameters, number of trees per acre, tree height, canopy height, and ground impedance are used as parameters in the PE model. A predicted C-4 spectrum is used to weight the starting field in the PE. Upwind and downwind cases are examined. The forest PE model is compared, using appropriate parameters, to both the forest and the open field measurements. Finally, the forest PE model is compared to the open field PE model for long distances, as a way to investigate differences in propagation through these distinctive settings.

Part I

Introduction

The forest is a highly complex acoustic medium. In attempting to understand it, one must consider the vertical sound speed profile, the ground impedance, and scattering from the trees. Previous attempts at modeling the forest have typically considered only two of the three major components, usually ground impedance and tree scattering, although more recent papers included only the vertical sound speed profile (see, for example, Swearingen [12], Albert [1], Tunick [13], and Heimann [9]). In this paper we present a model that incorporates all three factors. The model is based on the GFPE algorithm. The model is used in two different ways, first to compare forested and open field propagation to experimental data, and then to compare forested to open field propagation. These comparisons are performed at 174 m and 1400 m, because these distances correspond to experimental receiver locations.

1

Part II
The Forest Model

As stated in the introduction, the model is based on the GFPE. Since that model is well described in the literature, the derivation will not be included here. Instead, the reader is referred to Gilbert [8] and Salomons [11], two excellent papers describing the GFPE. The following sections will describe the geometry, vertical sound speed profile, ground impedance, trunk and canopy scattering, and the blast spectrum.

1 Geometry

The geometry of this model is based on measurements taken in the field test. This dictates that the forest height be 15 m, and the canopy begins at 10 m above the ground. While the trunk and canopy sizes and spacings are variable within the model itself, they are set to match the measurements taken in the field. The source height was 2 m above the ground, and, for the spectra, the receiver height is 1.2 m above the ground. Trunk cylinders are randomly spaced, but all perpendicular to the ground, and extend to the top of the canopy. The canopy is also made up of cylinders, which are oriented parallel to the trunks. They extend from the bottom of the canopy to the top of the canopy. Only two estimated branch sizes are considered. Figure 1 is a graphical interpretation of the model.
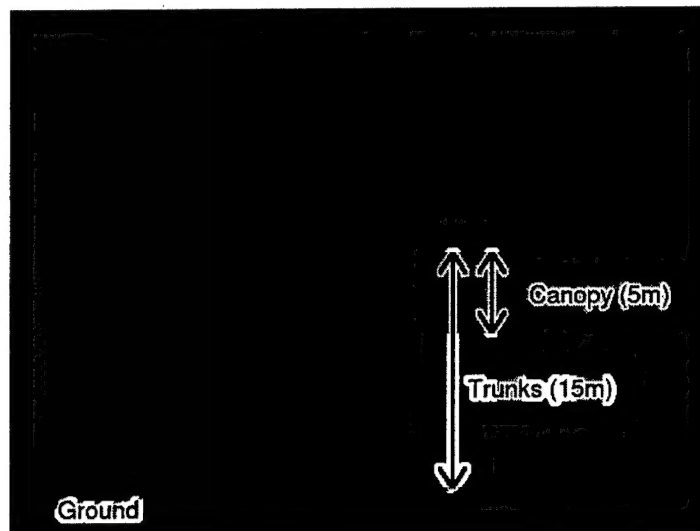

Figure 1: Geometry of the model

2 Atmospheric Variation with Height

The atmosphere near the ground surface exchanges heat with the surface and loses speed due to viscous drag. This drag causes shear in the wind profile and is the major generator of mechanical turbulence. Depending on the surface heating, the wind speed variation with height above the boundary can take one of several forms. An excellent recent summary of the situation has been published by Wilson [15].

The presence of the forest canopy serves as a target for solar heating, causing the ground to be partly shaded. In the absence of solar heating, radiative cooling within the canopy is reduced as well, because the upper canopy is at a much higher temperature than the open night sky. The presence of trees appears to the wind as additional roughness elements, increasing the drag. Because leaf areas, heat capacities, and transpiration of the various surfaces differ widely between tree types, the detailed microclimate within the forest is complex. Tunick[13] has developed a two-dimensional model for this problem.

In order to understand refraction of traffic noise beyond a grove of trees, Heimann[9] implemented a 3-D computational fluid dynamical model for the flow past a random assembly of truncated vertical right circular cylinders. The supposed incident flow field consisted of a wind profile with logarithmic variation with height. After passing through the grove of trees, the mean flow at mid-height of the canopy was reduced and nearly constant with height. Near the top of the canopy was a strong wind shear, with wind increasing a bit more than the incident wind at that height. Above the canopy, the difference between forest wind and open field wind grew smaller.

Because the incident open field wind and the forest wind profiles result from the same impressed wind field, they offer a foundation for comparative assessment of wind refraction. We chose to use the wind fields as computed by Heimann[9] as a starting point for examining the basic effect of wind refraction of sound by forest and open field. We scaled the wind profiles by height to match the canopy height in our experimental measurement, and extended the published profiles to smoothly converge to same wind speed at 40 m height, and to conserve total horizontal flow. Note that just above the canopy top, the comparative increase of wind speed above the open field value is required to balance the surplus of incident wind from the open field at the canopy height and below. The scaled wind profiles are shown in Figure 2.

Of course, left unaccounted for by this scaling were adjustments for the tree stand densities and the leaf area indices. We have also omitted the temperature dependence of the problem by setting the temperature to a constant. Nevertheless, the strengths of the gradients are appropriate for *some* value of imposed flow. Additionally, the larger wind profile gradients coincide with the ground surface and canopy top, as would temperature gradients resulting from surface radiative heat transfer.
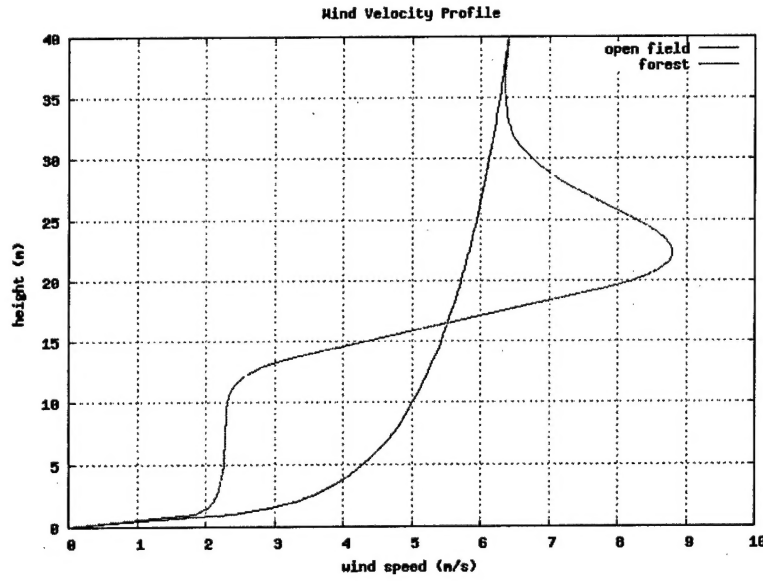
Figure 2: Model wind profiles for forest and open field

3   Ground Impedance

Ground impedance under the tree canopy is typically affected most by the detritous composing the surface layer. The ground impedance was not directly measured. Instead, the measured receiver spectrum at short range ($< 80\,\mathrm{m}$ from the source) was compared to a forward prediction using a van der Pol-type solution for a homogeneous half-space above porous ground. The ground impedance was modeled with a simple function developed by Attenborough [3], providing a reasonable match to the receiver spectrum. The ground "dip" in the spectrum was fairly easy to obtain by adjusting effective flow resistivity until good fit to the receiver spectrum was achieved.

Within the trees, the porous surface was made up of a layer of pine straw ($3\,\mathrm{cm}$), above a very thin ($< 0.3\,\mathrm{cm}$) layer of highly-decomposed pine straw. Below this was a fairly-consolidated sand layer (with no evidence of decomposed straw), which was modeled as a hard-backing.

In the open field, a mixture of thick grasses ($1\,\mathrm{m}$ high) and blackberry bushes ($1\,\mathrm{m}$ high), overlaid a spongy surface atop clay. A few points on the surface were saturated with water; others were dry. The surface was sloped approximately 1 to 2 degrees transverse to the direction of propagation.

The characteristic impedance of the porous surface layer is calculated from $Z_c = \omega \rho_b / k_b$, as a fluid having complex-valued bulk density and wavenumber,

$$\rho_b = \frac{4T}{3\Omega} + i\frac{4\Omega \sigma_e}{\omega \rho}$$

and

$$k_b = \gamma^{1/2} \left[\rho_b \Omega - \left(1 - \frac{1}{\gamma}\right) N_{\mathrm{Pr}} T \right]^{1/2}$$

where T is tortuousity, Ω is volume porosity ($\mathrm{m^3/m^3}$), ω is angular frequency ($\mathrm{rad/s}$), ρ is air density ($\mathrm{kg/m^3}$), γ is the ratio of specific heat capacities, and N_{pr} is the Prandtl number.

This ground surface corresponds to Attenborough's three parameter homogeneous (H3A) model. Finally, using the H3A model for a thin upper layer where porosity decreases with depth, and with hard backing, leads to

$$Z/\rho c = (Z_c/\rho c) + i/\left(2\gamma \omega \rho \Omega d\right)$$

4

where c is the speed of sound in air (m/s), and d is the depth of the surface layer (m).

The parameters used for evaluating ground impedance with the H3A model were $\rho = 1.2$, $c = 350$, $\gamma = 1.4$, and $N_{\mathrm{Pr}} = 0.724$. For pine forest: $\sigma_e = 7.5\,\mathrm{kPa} \cdot \mathrm{s} \cdot \mathrm{m}^{-2}$, $d = 0.03\,\mathrm{m}$, $\Omega = 0.4$, and $T = 2.0$. For open field, $\sigma_e = 57\,\mathrm{kPa} \cdot \mathrm{s} \cdot \mathrm{m}^{-2}$, $d = 0.053\,\mathrm{m}$, $\Omega = 0.4$, and $T = 2.0$.

4 Trunk and Canopy Scattering

The trunk and canopy scattering are both based on Twersky's multiple scattering model (see, for example Twersky [14] or Embleton [5]). In both the trunk and canopy cases, the approximation of infinite cylinders is used, scaled appropriately for size and number density of scatterers. The number and size of tree trunks are taken from the measurements. The number density of trees is $0.0124\,\mathrm{m}^{-1}$ and the average tree radius is $0.0925\,\mathrm{m}$. The canopy is approximated by large and small branches. These are scaled in size and number from the tree trunk parameters. The large branches are assumed to be 1/3 of the trunk radius and six times the number of trunks. The small branches are assumed to be 1/8 of the trunk radius and 24 times the number of trunks.

The result of Twersky's multiple scattering model for randomly placed parallel infinite cylinders is a complex effective bulk propagation wavenumber, k_s, where

$$k_s = \sqrt{k_0^2 - 4iNg + (g'^2 - g^2)(2N/k_0)^2}$$

and $k_0 = \omega/c_0$ is the unobtruded wavenumber, N is the number of trees per meter, and g and g' are the forward and backward scattering coefficients, respectively, defined as

$$g = \sum_{n=0}^{\infty} A_n$$
$$g' = \sum_{n=0}^{\infty} (-1)^n A_n$$
$$A_n = \frac{-iJ_n(k_0 a) + Z_w J_n'(k_0 a)}{iH_n^{(1)}(k_0 a) + Z_w H_n^{(1)\prime}(k_0 a)}$$

and Z_w is the surface impedance of the tree. In this case, Z_w is nearly rigid, following Price[10]. Plots of the real and imaginary parts of k_s are included in Figure 3.

The scattering is implemented in the GFPE by adjusting the wavenumber in the appropriate regions. For the trunk scattering, the wavenumber is adjusted from the ground to the tree top height, or $0\,\mathrm{m}$ to $15\,\mathrm{m}$. The canopy begins at $10.6\,\mathrm{m}$. To incorporate the canopy scattering, the imaginary parts of the bulk scattering wavenumbers due to the large and small branches are added to the trunk scattering wavenumber. This is possible because the real part of the wavenumbers are constant within 0.02%, and are therefore considered negligible differences (see Figure 4).

While the scattering effect is small over short distances and for low frequencies, it increases significantly with both frequency and distance. Figure 5 shows the attenuation per unit thickness due to scattering in units of $\mathrm{dB}/100\,\mathrm{m}$. The plot shows that attenuation increases with frequency, as expected, and that it has a greater overall effect than atmospheric absorption.

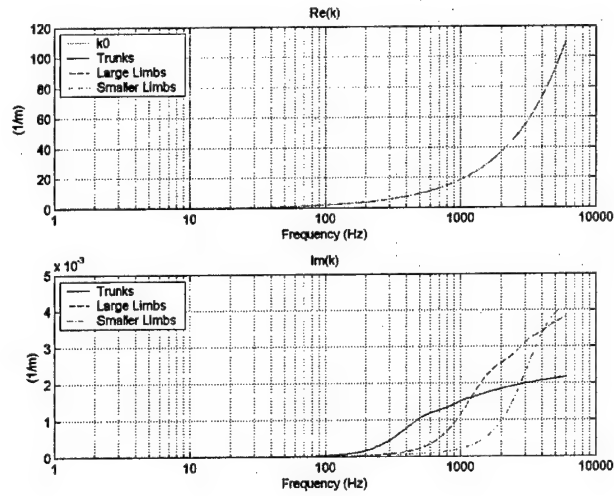$$A_{tree} = 20 \cdot \mathrm{Im}(k_s) \cdot dist / \log_{10}(e) \ (\mathrm{dB}) \tag{1}$$

Figure 3: Real and imaginary parts of k_s plotted as a function of frequency
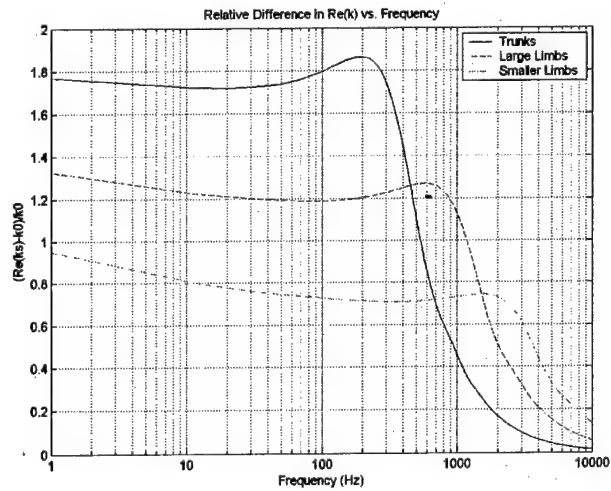

Figure 4: Relative differences between scattering wavenumbers and unobtruded wavenumber
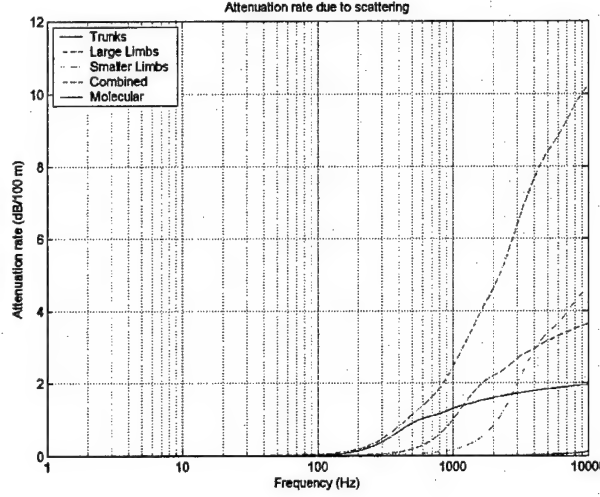
6

Figure 5: Attenuation rate due to scattering, in dB/100 m

5 Blast Wave Spectrum

Explosions of Composition C-4 were employed as the sound source. The use of C-4 provided a high-pressure, broadband, compact, isotropic source with fairly repeatable event-to-event sound energy. The charges were formed into spheres, each wrapped with a thin plastic bag and suspended by a rope so that their centers were approximately 2 m above the surface. The sound wave produced by an explosion in air has been modeled extensively. It is convenient to approximate the sound pressure-time history with an expression due to Friedlander [7],

$$p_t = p^0 \left(1 - \frac{t}{t_d}\right) \exp\left(-t/t_d\right) \Theta_t \tag{2}$$

where p^0 is the peak positive overpressure (Pa), t_d is the positive phase duration (s), and Θ is the Heaviside step operator.

Although the waveform fails to indicate the finite rise time of the shock, or to show pulse broadening or rounding that result from attenuation and temporal dispersion, it offers a simple starting point for spectral analysis. Its Fourier transform is,

$$\widetilde{p}_f \equiv \int_{-\infty}^{\infty} p_t e^{-i\omega t} \mathrm{d}t = p^0 t_d \left(-i\omega t_d\right)/\left(1 + i\omega t_d\right)^2 \tag{3}$$

where $\omega = 2\pi f$ is the angular frequency, and it has the corresponding sound exposure spectrum,

$$\widetilde{E}_f = 2\left(p^0 t_d\right)^2 \omega^2 t_d^2 / \left(1 + \omega^2 t_d^2\right)^2. \tag{4}$$

This function has its maximum value at $\omega = 1/t_d$.

For the (admittedly unrealistic) homogeneous and unbounded field at 1 km distance from a 1 kg charge of Composition C-4, $p_{1\,\mathrm{kg}}^0 = 79\,\mathrm{Pa}$ and $t_{d,1\,\mathrm{kg}} = 0.0089\,\mathrm{s}$. For other charge sizes, it generally holds that the pressure and duration increase according to the cube root of charge weight, $p_x^0/p_{1\,\mathrm{kg}}^0 = (W_x/1\,\mathrm{kg})^{1/3}$ and $t_{d,x}/t_{d,1\,\mathrm{kg}} = (W_x/1\,\mathrm{kg})^{1/3}$, although more accurate expressions appear in ANSI S2.20[2] and Ford *et al.* [6].

Figure 6 shows the spectrum of a C-4 explosion at 1 km in an unbounded field, evaluated for the two charge sizes employed in the measurement, 0.57 kg and 2.27 kg. Both narrow band (1 Hz bandwidth) and 1/3-octave spectra are shown. Also shown are curves calculated by adding $10\lg\left(f_c/1\,\mathrm{Hz}\right) - 6.36\,\mathrm{dB}$ to the narrow band sound exposure levels. These latter curves are shown to enable rough comparison to 1/3-octave band spectra.

7

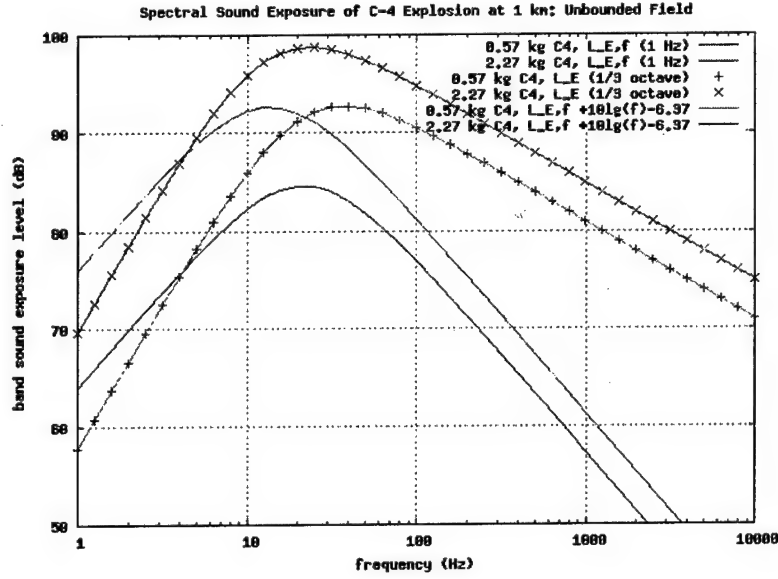**Spectral Sound Exposure of C-4 Explosion at 1 km: Unbounded Field**

Figure 6: Idealized sound exposure spectrum of Composition C-4 explosion at 1km distance in an unbounded homogeneous atmosphere

6 The Forest GFPE

The previous sections all described the components of the forest GFPE model. This section contains example plots of the resulting model. The model was calculated for both upwind and downwind propagation over a range of frequencies from 1 Hz to 2200 Hz. The figures below are snapshots taken at 40 Hz, 400 Hz, and 1000 Hz. In all of the figures, the source is located at 2 m above the ground, and is assumed to be a unit source with an analytic starting field, as shown below. The form of the starting field follows that in Cooper[4]

$$
\phi(r_s, z) = \begin{cases}
\sqrt{r_s}\{\frac{e^{jkR_1}}{R_1} + \frac{e^{jkR_2}}{R_2}[R_p + (1-R_p)F_1]\}, & 0 \le z \le z_s \\
\sqrt{r_s}\{\frac{e^{jkR_1}}{R_1} + \frac{e^{jkR_2}}{R_2}[R_p + (1-R_p)F_1]\} & \\
\quad \times [\frac{1}{2}(\cos(\frac{(z-z_s)\pi}{z_{attn}-z_s}) + 1)], & z_s < z < z_{attn} \\
0, & \text{otherwise}
\end{cases}
$$

where $r_s = 0 + dr$, $R_1 = \sqrt{(r_s)^2 + (z-z_s)^2}$, $R_2 = \sqrt{(r_s)^2 + (z+z_s)^2}$, R_p is the plane wave reflection coefficient, given by

$$R_p = (\sin\phi - \beta_g)/(\sin\phi + \beta_g)$$

where β_g is the normalized acoustical admittance of the ground surface, $\beta_g = 1/Z_g$, and

$$
\begin{aligned}
F_1 &= 1 + j\sqrt{\pi}\Lambda e^{-\Lambda^2}\,\text{erfc}(-j\Lambda) \\
\Lambda &= \sqrt{ikR_2}\sqrt{1 + \beta_g \sin\phi - (1-\beta_g^2)^{1/2}\cos\phi}
\end{aligned}
\tag{5}
$$

where ϕ is the acute angle subtended by R_2 and the ground, and F_1 represents the first term in the asymptotic expansion solution of the spherical wave reflection coefficient.

In all of the figures, notice that the forest appears to be "trapping" energy below the canopy. This effect is much more pronounced in the downwind cases. Shown below are the following: 40 Hz in Figure 7, 400 Hz in Figure 8, and 1000 Hz in Figure 9.

We will next examine the relative contributions of each component of the model by starting with only the atmospheric profile present, and then adding additional components. This has been done in Figures 10

8

and 11, both upwind and downwind cases. Looking at the 174 m location, the ground effect is large, and the scattering components are only roughly a 2 dB contribution at 1000 Hz. At the 1400 m location, the ground effect is again large, but the scattering is now much more significant, especially above around 400 Hz.
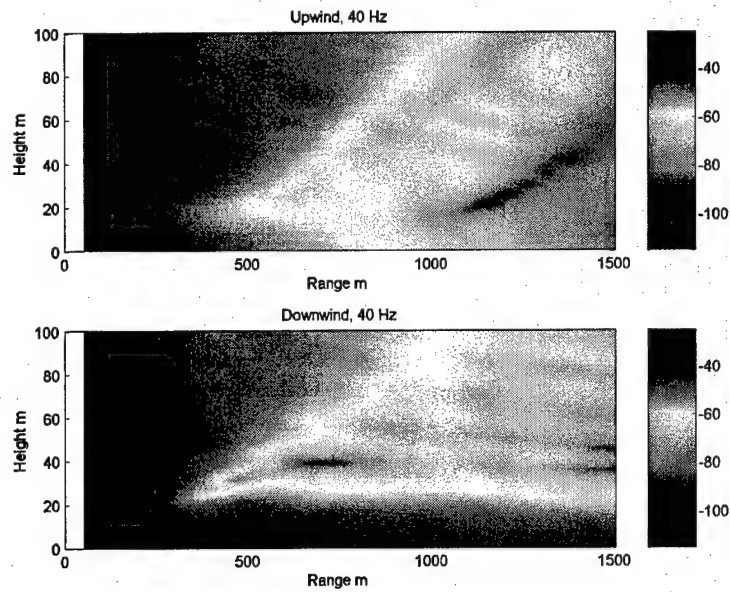

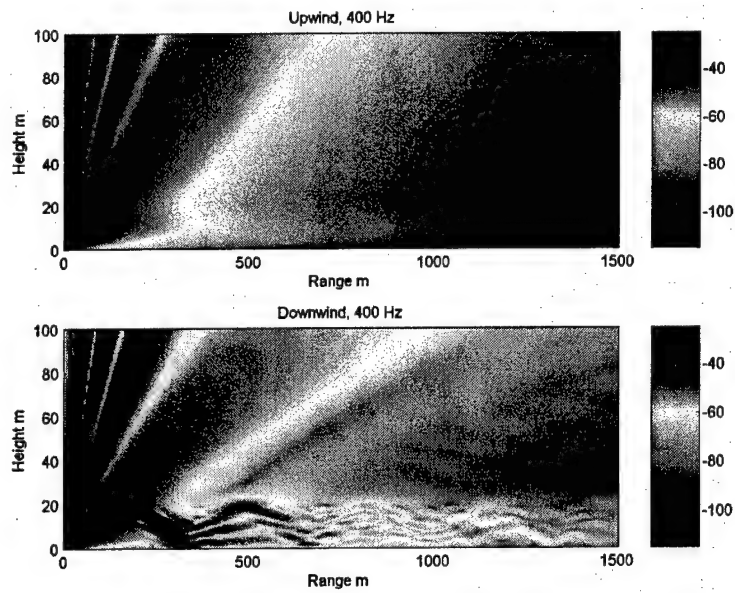Figure 7: Forest GFPE at 40 Hz, upwind and downwind cases.

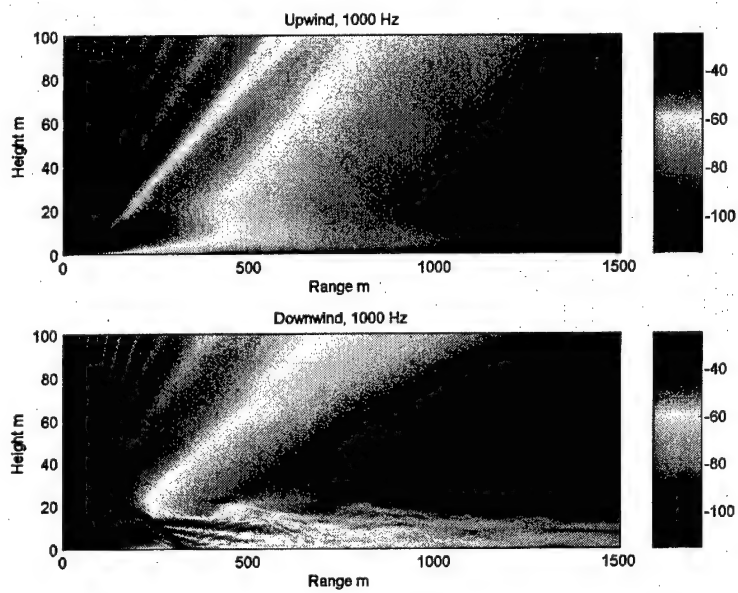Figure 8: Forest GFPE at 400 Hz, upwind and downwind cases.

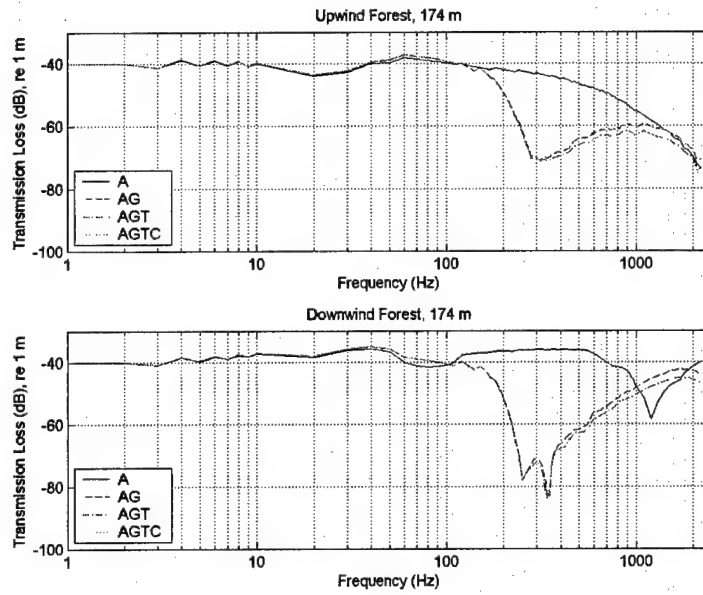Figure 9: Forest GFPE at 1000 Hz, upwind and downwind cases.

10

Figure 10: Buildup of model components, 174 m location. In the legend, A=Atmospheric Profile, G=Ground Effect, T=Trunk Scattering, C=Canopy Scattering.
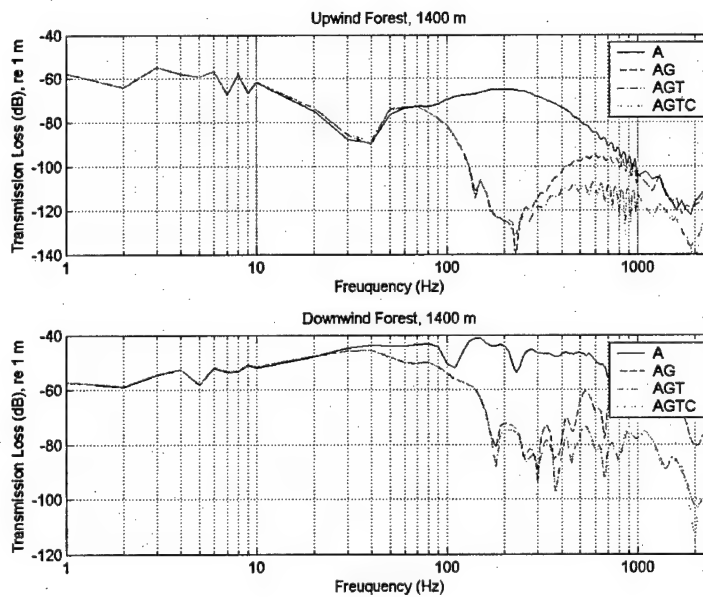

Figure 11: Buildup of model components, 1400 m location. In the legend, A=Atmospheric Profile, G=Ground Effect, T=Trunk Scattering, C=Canopy Scattering.

11

Part III

Analysis

The forest GFPE has been analyzed two different ways: by comparisons to data and comparisons between forest and open field. These comparisons are performed in both short (174 m) and long (1400 m) range regimes.

7   Comparisons to Data

Comparing theoretical predictions to field data can lead to interesting observations about both the prediction and the field test. In this case, data from a open field-forest experiment was available. In the experiment, two sizes of Composition C-4 were detonated at a height of 2 m above the ground, from four different locations. There were two source locations in the open field and just along the edge of the forest. The only data used here was taken in an open field at a distance of 174 m from one open field source, in the forest 174 m from one forest source, and in the forest 1400 m from one forest source. In all cases, the measured data is presented in 1/3 octave band SEL. The prediction spectra are weighted by the appropriate blast source spectrum.

Figure 12 shows the comparison between the forest GFPE calculations and the measured forest propagation data at 174 m from the source. At short range, the results are heavily dependent on assumptions we have made about the source. It is possible that the source spectrum used is not the most appropriate one. The measured data is generally higher in level than the predictions. The ground effect in the model is more pronounced than in the measurements. However, the general shapes match reasonably well. The ground dip and maximum value both appear at the proper frequencies. Further improvements are anticipated with adjustments to parameters, such as ground impedance.

Figure 13 shows the comparison between the field GFPE calculations and the measured open field propagation data. Again, at short range, the model results are heavily dependent on the source model. The apparent ground dip in the downwind prediction is not seen in the measurement.

Figure 14 shows the 1.25 lb C-4 case for a fully forested propagation path at 1400 m. After more careful analysis of the measured data, we determined that the spectrum in this comparison is likely to be anomalously low in level. This conclusion was derived from the fact that most of the long range data was uncalibrated or electronically clipped and could not be used due to equipment errors. The measured spectrum shown is from an un-clipped signal, and is therefore likely to be a lower level than the others. However, it is important to notice that the general shape of the spectrum matches reasonably well with the predicted spectra.
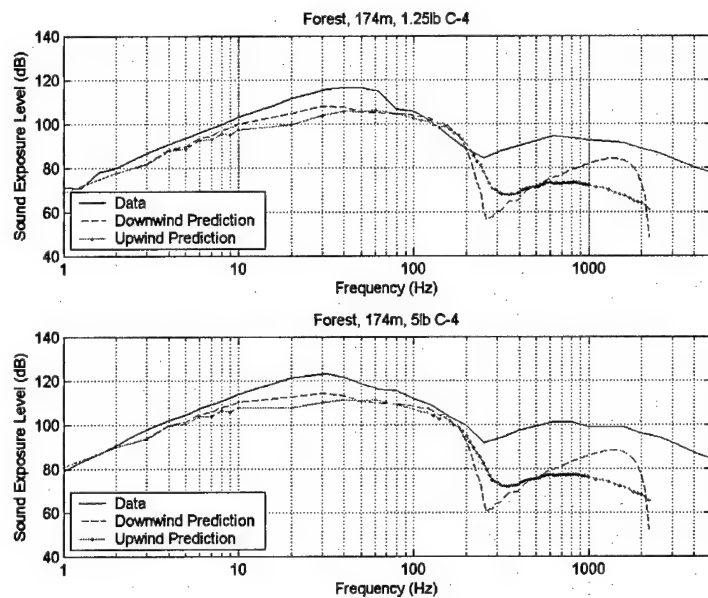
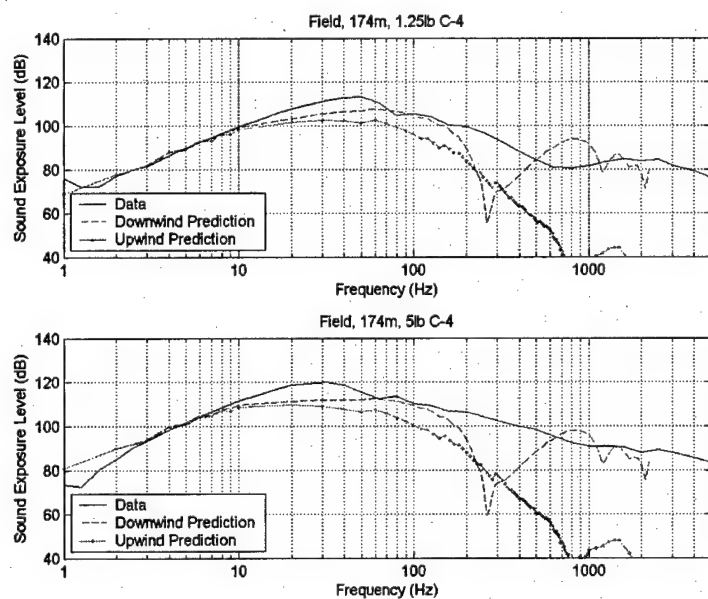Figure 12: Comparison of forest measurements to GFPE model, 174 m.

Figure 13: Comparison of open field measurements with GFPE model, 174 m.
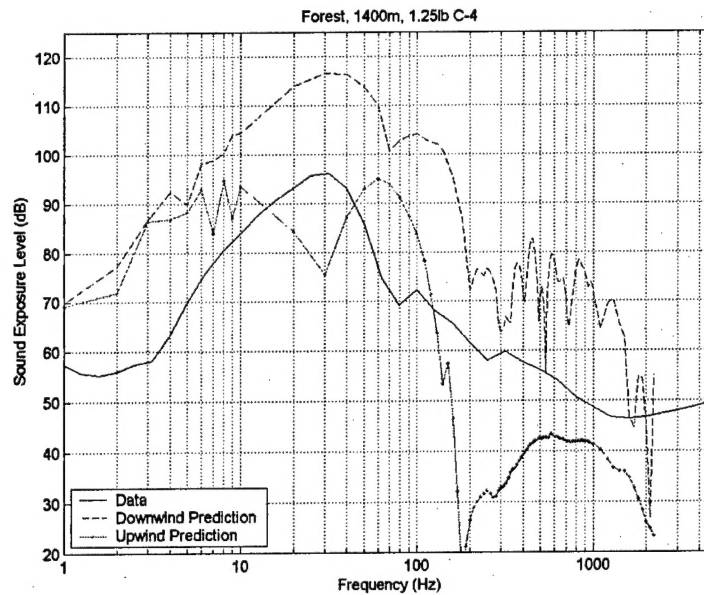
13

Figure 14: Comparison of forest measurements to GFPE model, 1400 m.

8   Forest vs. Field Comparisons

The original intent of the development of this model was to determine whether the presence of a forest around a noise source actually helped to mitigate noise. One way to get at this information from the model is to compare open field predictions to forest predictions. Figure 15 shows the difference in level between open field and forest predictions. If the resulting difference is positive, the open field is a better propagation medium over that frequency range. If the resulting difference is negative, the forest is a better propagation medium over that frequency range. It is important to note that the model does not include atmospheric turbulence. Omitting atmospheric turbulence causes the open field upwind cases to develop a strong shadow zone that would be somewhat lessened in a real setting.

From the comparison plots in Figure 15, several conclusions can be drawn. In the short range (174 m) downwind case, the forest is beneficial above 200 Hz, by an average of 8 dB. Between 45 and 100 Hz, there is a slight benefit (1-2 dB) from the forest. Below 45 Hz, the forest is a better propagating medium than the open field. In the short range (174 m) upwind case, with the exceptions of 20 Hz and 300 Hz, the open field is more beneficial in terms of noise mitigation. In the long range (1400 m) downwind case, the forest is beneficial for mitigation above 200 Hz, on the order of 8-10 dB on average, and anywhere from 0-20 dB. Below 200 Hz at long range downwind, the open field causes 3-11 dB more attenuation than the forest. In the upwind case, the forest is more beneficial for mitigation below 35 Hz, significantly worse between 35 Hz and 150 Hz, and then nominally more attenuating than the open field above 150 Hz.
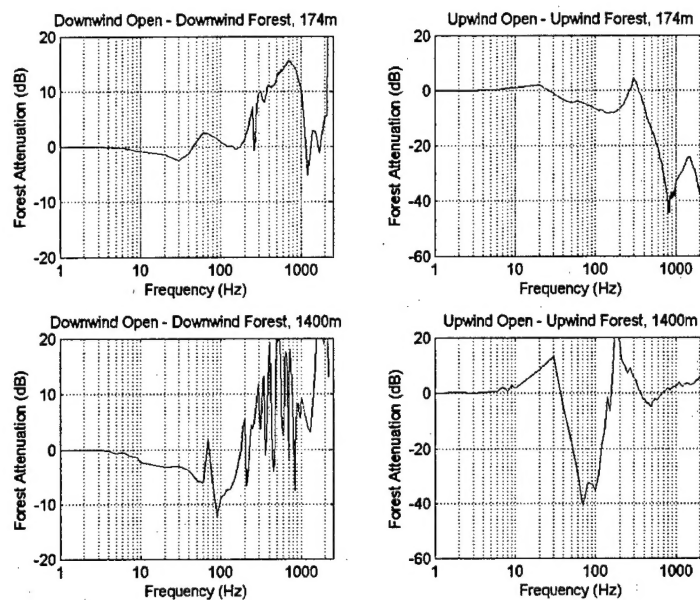
14

Figure 15: Relative attenuation of forest vs. open field.

Part IV
Conclusions and Future Work

Overall, the forest GFPE matches data taken in the forest and the open field in shape and trend, although not in magnitude. Although the levels are not exactly predicted, the general shapes of the spectra are close, especially in the long range. Possible sources of error include the choice of the Friedlander spectrum to weight the predictions, the values used for ground impedance, and the atmospheric profile used. More analysis is needed, including an assessment of the model's sensitivity to various parameters.

Because only one case has been examined here, it is difficult to draw general conclusions about the effectiveness of a forest for noise mitigation. However, for the set-up presented here, the upwind open field case produces the lowest levels across almost all frequencies tested, and at both short range (174 m), and at long range (1400 m), with the primary exception located near 300 Hz, which corresponds to the ground dip in the forest. Again, it is important to point out that turbulence has been neglected in all cases. When comparing downwind cases, the open field is slightly more attenuating than the forest for frequencies below 50 Hz in the short range, with the forest providing more attenuation above 50 Hz. In the long range, the forest provides more attenuation above roughly 200 Hz.

In the future, we plan to improve the atmospheric profile, perform sensitivity testing on atmospheric, ground impedance and scattering parameters. An important remaining challenge is to incorporate the incoherent field effects composing the backscatter and reverberation signals.

References

[1] DONALD G. ALBERT. Past research on sound propagation through forests. Tech Report xx, ERDC, Hanover, NH (2004).

[2] ANSI. "Standard for Estimating Airblast Characteristics for Single Point Explosions in Air, with a Guide to Evaluation of Atmospheric Propagation and Effects". Number S2.20-1983 (R1989) (ASA20) in

American National Standards. Acoustical Society of America, New York (1983). ANSI Working Group S2/WG54.

[3] KEITH ATTENBOROUGH. Ground parameter information for propagation modeling. *Journal of the Acoustical Society of America* **92**(1), 418–427 (1992).

[4] JENNIFER L. COOPER. "Parameter selection in the Green's Function Parabolic Equation for outdoor sound propagation over varied terrain". PhD thesis, The Pennsylvania State University (2003).

[5] T. F. W. EMBLETON. Scattering by an array of cylinders as a function of surface impedance. *Journal of the Acoustical Society of America* **40**(3), 667–670 (1966).

[6] ROY D. FORD, DAVID J. SAUNDERS, AND GEOFFREY KERRY. The acoustic pressure waveform from small unconfined charges of plastic explosive. *J. Acoust. Soc. Am.* **94**(1), 408–417 (July 1993).

[7] FREDERICK G. FRIEDLANDER. The diffraction of sound pulses. *Proc. R. Soc. London, Ser. A* pages 322–367 (1946).

[8] KENNETH E. GILBERT AND XIAO DI. A fast Green's function method for one-way sound propagation in the atmosphere. *Journal of the Acoustical Society of America* **94**(4), 2343–2352 (1993).

[9] DIETRICH HEIMANN. Numerical simulations of wind and sound propagation through an idealised stand of trees. *Acta Acoustica* **89**, 779–788 (2003).

[10] M. A. PRICE, K. ATTENBOROUGH, AND N. W. HEAP. Sound attenuation through trees: Measurements and models. *Journal of the Acoustical Society of America* **84**, 1836–1844 (1988).

[11] ERIK M. SALOMONS. Improved Green's function parabolic equation method for atmospheric sound propagation. *Journal of the Acoustical Society of America* **104**(1), 100–111 (1998).

[12] MICHELLE SWEARINGEN, DAVID SWANSON, AND KARL REICHARD. Survey of research of sound propagation in forests. In "Eighth International Symposium on Long-Range Sound Propagation", pages 131–138 (September 1998).

[13] ARNOLD TUNICK. Calculating the micrometeorological influences on the speed of sound through the atmosphere in forests. *J. Acoust. Soc. Am.* **114**(4), 1796–1806 (October 2003).

[14] VICTOR TWERSKY. On scattering of waves by random distributions. I. Free-space scatterer formalism. *Journal of Mathematical Physics* **3**(4), 700–715 (1962).

[15] D. KEITH WILSON. The sound speed gradient and refraction in the near-ground atmosphere. *J. Acoust. Soc. Am.* **113**(2), 750–757 (February 2003).

REPORT DOCUMENTATION PAGE

Form Approved
OMB No. 0704-0188

1. REPORT DATE (DD-MM-YYYY) 11-2004	2. REPORT TYPE Final	3. DATES COVERED (From - To)

4. TITLE AND SUBTITLE
Sound Propagation Through a Forest:
A predictive model

5a. CONTRACT NUMBER

5b. GRANT NUMBER

5c. PROGRAM ELEMENT NUMBER

6. AUTHOR(S)
Michael White and Michelle Swearingen

5d. PROJECT NUMBER
622720A896

5e. TASK NUMBER

5f. WORK UNIT NUMBER

7. PERFORMING ORGANIZATION NAME(S) AND ADDRESS(ES)
U.S. Army Engineer Research and Development Center (ERDC)
Construction Engineering Research Laboratory (CERL)
PO Box 9005
Champaign, IL 61826-9005

8. PERFORMING ORGANIZATION REPORT NUMBER
ERDC/CERL MP-04-3

9. SPONSORING / MONITORING AGENCY NAME(S) AND ADDRESS(ES)
U.S. Army Center for Health Promotion and Preventive Medicine
5158 Blackhawk Road
APG, MD 21010-5403

10. SPONSOR/MONITOR'S ACRONYM(S)
USACHPPM

11. SPONSOR/MONITOR'S REPORT NUMBER(S)

12. DISTRIBUTION / AVAILABILITY STATEMENT
Approved for public release; distribution is unlimited.

13. SUPPLEMENTARY NOTES
Copies are available from the National Technical Information Service, 5285 Port Royal Road, Springfield, VA 22161.

14. ABSTRACT

Previous attempts at modeling sound propagation through a forest have largely neglected the effects of a sound speed profile. This paper presents a PE-based sound propagation model that includes forest effects. In addition to a simplified but realistic sound speed profile, the model includes ground impedance effects, bulk attenuation due to multiple scattering by tree trunks and canopy, and the usual spherical spreading and atmospheric absorption.

15. SUBJECT TERMS
Sound propagation modeling, forests, sound speed profile, predictive modeling, sound mitigation

16. SECURITY CLASSIFICATION OF:			17. LIMITATION OF ABSTRACT	18. NUMBER OF PAGES	19a. NAME OF RESPONSIBLE PERSON Michael J. White
a. REPORT Unclassified	b. ABSTRACT Unclassified	c. THIS PAGE Unclassified	SAR	22	19b. TELEPHONE NUMBER (include area code) (217) 352-6511

NSN 7540-01-280-5500

Standard Form 298 (Rev. 8-98)
Prescribed by ANSI Std. 239.18